

CPA for charge ordering in the extended Hubbard model

A. T. Hoang^{1,2} and P. Thalmeier³

¹ *Max-Planck-Institut für Physik komplexer Systeme, Nöthnitzer Strasse 38, 01187 Dresden, Germany*

² *Institute of Physics, P.O.Box 429 Bo Ho, Hanoi 10000, Vietnam*

³ *Max-Planck-Institut für Chemische Physik fester Stoffe, Nöthnitzer Strasse 40, 01187 Dresden, Germany*
(December 25, 2021)

We study charge ordering in the extended Hubbard model with both on-site and nearest neighbor Coulomb repulsion (U and V , respectively) within the Coherent potential approximation (CPA). The phase boundary between the homogeneous and charge ordered phase for the square lattice is obtained for different values of U . It is shown that at quarter filling for all values of U the charge ordering exists only if the inter-site Coulomb repulsion V exceeds certain critical value which is of the order of the kinetic energy t . At finite temperature a reentrant transition is found in some region of V .

PACS 71.10.Fd, 71.27.+a

I. INTRODUCTION

The problem of charge ordering (CO) attracted the attention of physicists already at the end of the thirties. In the low density limit, as was first proposed by Wigner¹, the electrons crystallize in form of a lattice in order to keep the Coulomb repulsion as small as possible. Such a Wigner lattice is experimentally realized in a GaAs/AlGaAs heterostructure². The CO may also occur at higher electron concentration if the interaction of electrons with spin degrees of freedom or with phonons drastically reduces the kinetic energy³. Recently the CO is extensively observed in real materials at high densities: hole ordering in rare-earth pnictides like Yb₄As₃⁴, charge ordering in the unconventional spin-Peierls material α' -NaV₂O₅⁵ and in colossal magnetoresistance compounds, for example in R_{2-2x}A_{1+2x}Mn₂O₇ (R = La, Pr; A = Ca, Sr; $x \geq 0.5$)⁶.

One of the simplest models of interacting electrons that allows for charge ordering is the extended Hubbard model (EHM). This model has been intensively studied both in low dimensions and in the limit of infinite dimension, usually at half or at quarter filling. A variety of techniques, such as Hartree-Fock approximation⁷, perturbation theory⁸, the dynamical mean field theory (DMFT)⁹, slave boson approach¹⁰, as well as numerical methods like Quantum Monte Carlo simulation¹¹ and Lanczos technique¹² have been employed. Obviously, each of these approaches is able to describe in a proper way only one of the relevant limits of the model and

despite many publications devoted to the CO in solids the physical picture of the phenomenon is far from being clear.

Recently a melting of the charge ordered state on decreasing the temperature has been found in the doped compounds Pr_{0.65}(Ca_{0.7}Sr_{0.3})_{0.35}MnO₃¹³ and La_{2-2x}Sr_{1+2x}Mn₂O₇ ($0.47 \leq x \leq 0.62$)^{14,15}. A reentrant transition at quarter filling has been obtained theoretically using EHM both with electron-phonon interaction¹⁶ and without electron-phonon interaction^{9,7}. The present paper is devoted to study of the boundary between the charge ordered and disordered phase for different regimes of the temperature T , the Coulomb interactions U, V and the band filling n . A simple but physically meaningful approximation allowing to solve this problem is the CPA. This self-consistent approximation is recognized as the best single-site approximation for the spectral properties of disordered systems. Originally, the alloy-analog approximation has been formulated as an approximation scheme for the Hubbard model¹⁷. To solve the alloy problem the CPA is used as a second step. The CPA was also applied to intermediate valence and heavy fermion systems¹⁸. In the present work this approximation is used for the first time to treat the charge ordering in the EHM.

II. MODEL AND FORMALISM

We consider the following Hamiltonian for the EHM:

$$H = t \sum_{\langle ij \rangle \sigma} (c_{i\sigma}^{\dagger} c_{j\sigma} + c_{j\sigma}^{\dagger} c_{i\sigma}) + U \sum_i n_{i\uparrow} n_{i\downarrow} + V \sum_{\langle ij \rangle} n_i n_j \quad (1)$$

where $c_{i\sigma} (c_{i\sigma}^{\dagger})$ annihilates (creates) an electron with spin σ at site i , $n_{i\sigma} = c_{i\sigma}^{\dagger} c_{i\sigma}$ and $n_i = n_{i\uparrow} + n_{i\downarrow}$. $\langle ij \rangle$ denotes nearest neighbors, t is the hopping parameter, U and V are on-site and inter-site Coulomb repulsion, respectively. We divide the hypercubic lattice in two sublattices such that points on one sublattice have only points of the other sublattice as nearest neighbors. The sublattice is denoted by subindex A or B: $c_{i\sigma} = a_{i\sigma} (b_{i\sigma})$ if $i \in A$ ($i \in B$). Performing a mean-field decoupling of the V term, we get

$$\begin{aligned}
H = & \sum_{i \in A, \sigma} zV n_B a_{i\sigma}^+ a_{i\sigma} + U \sum_{i \in A} n_{i\uparrow} n_{i\downarrow} + \\
& \sum_{j \in B, \sigma} zV n_A b_{j\sigma}^+ b_{j\sigma} + U \sum_{j \in B} n_{j\uparrow} n_{j\downarrow} \\
& + t \sum_{\langle ij \rangle \sigma} (a_{i\sigma}^+ b_{j\sigma} + b_{j\sigma}^+ a_{i\sigma}) - \frac{1}{2} zNV n_A n_B
\end{aligned} \quad (2)$$

where z is the number of nearest neighbors, $n_{A/B}$ is the averaged electron occupation number in the A/B-sublattice, N is the number of sites in the lattice. In the alloy-analog approach the many-body Hamiltonian (2) is replaced by a one-particle Hamiltonian with disorder which is of the form

$$\begin{aligned}
H = & \sum_{i \in A, \sigma} E_{A\sigma} a_{i\sigma}^+ a_{i\sigma} + \sum_{j \in B, \sigma} E_{B\sigma} b_{j\sigma}^+ b_{j\sigma} \\
& + t \sum_{\langle ij \rangle \sigma} (a_{i\sigma}^+ b_{j\sigma} + b_{j\sigma}^+ a_{i\sigma}) - \frac{1}{2} zNV n_A n_B
\end{aligned} \quad (3)$$

where

$$E_{A/B, \sigma} = \begin{cases} zV n_{B/A} & \text{with probability } 1 - n_{A/B, -\sigma} \\ zV n_{B/A} + U & \text{with probability } n_{A/B, -\sigma} \end{cases} \quad (4)$$

In the following we assume spin-independent expectation values in (4), i.e. we consider only nonmagnetic solution: $n_{\alpha\uparrow} = n_{\alpha\downarrow} = \frac{1}{2} n_\alpha$; ($\alpha = A, B$). The Green function G corresponding to the Hamiltonian (3) has to be averaged over all possible configurations of the random potential which can be considered to be due to alloy constituents. The averaging cannot be performed exactly. To solve the alloy problem the CPA is used. The averaged Green function \bar{G} is obtained from an effective Hamiltonian containing a self-energy $\Sigma_{A/B}(\omega)$ for the A/B-sublattice:

$$\begin{aligned}
H_{eff} = & \Sigma_A(\omega) \sum_{i \in A, \sigma} a_{i\sigma}^+ a_{i\sigma} + \Sigma_B(\omega) \sum_{j \in B, \sigma} b_{j\sigma}^+ b_{j\sigma} \\
& + t \sum_{\langle ij \rangle \sigma} (a_{i\sigma}^+ b_{j\sigma} + b_{j\sigma}^+ a_{i\sigma})
\end{aligned} \quad (5)$$

In momentum space the averaged Green functions $\bar{G}_{A/B}(\vec{k}, \omega)$ for the A/B-sublattice are of the form

$$\bar{G}_A(\vec{k}, \omega) = \left(\omega - \Sigma_A(\omega) - \frac{t_k^2}{\omega - \Sigma_B(\omega)} \right)^{-1} \quad (6)$$

$$\bar{G}_B(\vec{k}, \omega) = \left(\omega - \Sigma_B(\omega) - \frac{t_k^2}{\omega - \Sigma_A(\omega)} \right)^{-1} \quad (7)$$

where t_k is the Fourier transform of the hopping matrix element (the wavevector \vec{k} is for sublattice A (or B)), $\Sigma_{A/B}(\omega)$ are to be determined latter. The density of states (DOS) for free electrons with the band dispersion t_k is replaced by the semi-elliptical

$\rho_0(\omega) = \frac{2}{\pi W^2} \sqrt{W^2 - \omega^2}$ (we set $W = 1$ as the unit for the energy scale). Note that this model DOS is often used as an additional approximation in combination with the CPA. It was noted in Ref.¹⁹ that for the Bethe lattice with $3 \leq z \leq 6$ this approximation is a good one, at least in a qualitative sense. The averaged Green functions $\bar{G}_{A/B}(\omega)$ for the A/B-sublattice then take the form

$$\begin{aligned}
\bar{G}_A(\omega) = & \frac{1}{N} \sum_{\vec{k}} \bar{G}_A(\vec{k}, \omega) = \frac{2}{W^2} \left(\omega - \Sigma_B(\omega) \right. \\
& \left. - \left[(\omega - \Sigma_B(\omega))^2 - \frac{\omega - \Sigma_B(\omega)}{\omega - \Sigma_A(\omega)} W^2 \right]^{1/2} \right)
\end{aligned} \quad (8)$$

And $\bar{G}_B(\omega)$ is obtained by replacing $A \leftrightarrow B$. A scattering matrix T is introduced for each configuration via

$$G = \bar{G} + \bar{G} T \bar{G} \quad (9)$$

The CPA demands that the scattering matrix vanishes on average: $\bar{T} = 0$. This yields expression for $\Sigma_{A/B}(\omega)$ of the form

$$\begin{aligned}
\Sigma_A(\omega) = & \bar{E}_A - (zV n_B - \Sigma_A(\omega)) \cdot \\
& \bar{G}_A(\omega) (zV n_B + U - \Sigma_A(\omega))
\end{aligned} \quad (10)$$

where $\bar{E}_A = zV n_B + \frac{1}{2} U n_A$. Again $\Sigma_B(\omega)$ and \bar{E}_B are obtained by replacing $A \leftrightarrow B$.

For arbitrary size of electron density n we make the following ansatz:

$$n_{A/B} = n \pm x; \quad \bar{G}_{A/B}(\omega) = G(\pm x, \omega)$$

Eliminating $\Sigma_A(\omega), \Sigma_B(\omega)$ from (8) and (10) leads to an equation for $G(\pm x, \omega)$:

$$\begin{aligned}
\omega - \frac{G(-x, \omega)}{4} - \frac{1}{G(x, \omega)} = & zV(n - x) + \frac{U}{2}(n + x) - \\
\left[zV(n - x) - \omega + \frac{G(-x, \omega)}{4} + \frac{1}{G(x, \omega)} \right] \cdot & \\
\left[zV(n - x) + U - \omega + \frac{G(-x, \omega)}{4} + \frac{1}{G(x, \omega)} \right] G(x, \omega) &
\end{aligned} \quad (11)$$

Setting $x = 0$ in eq.(11) and shifting the one-electron energy by $zVn + \frac{U}{2}$ we reproduce the CPA equation for the Green function obtained by Velicky et al in Ref.²⁰. If μ is the chemical potential of electrons, then at the temperature T one has

$$\begin{aligned}
n_\alpha = & \frac{2T}{N} \sum_{\vec{k}, n} \bar{G}_\alpha(\vec{k}, i\omega_n) \\
= & -\frac{2}{\pi} \int_{-\infty}^{+\infty} d\omega f(\omega) \Im G(n_\alpha - n, \omega)
\end{aligned} \quad (12)$$

where $\omega_n = (2n + 1)\pi T$ is the Matsubara frequencies and $f(\omega) = (1 + \exp(\omega - \mu)/T)^{-1}$ is the Fermi function. The pair of equations (12) must now be solved with the

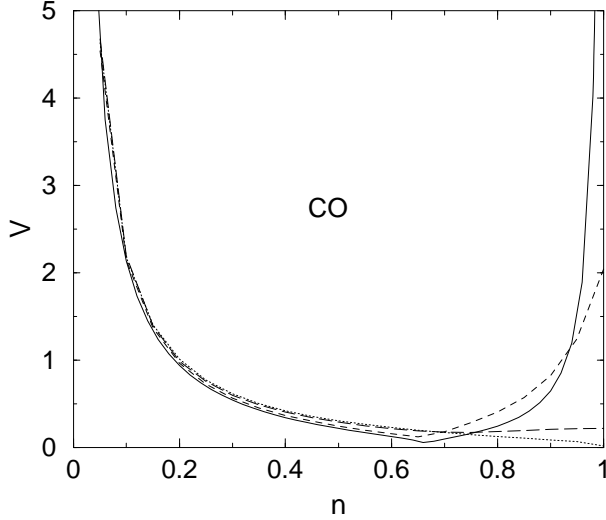


FIG. 1. $(V-n)$ -phase diagram for the 2D extended Hubbard model ($W = 1$, $T = 0$) for different values of U : $U = 0, 0.5, 1.5$ and $U = \infty$ corresponding to the dotted, long-dashed, dashed and solid lines, respectively.

constraint $n_A + n_B = 2n$ for n_A, n_B and μ . For small enough V the solution of (12) is the charge disordered state with $n_A = n_B$. But if V is sufficiently large it may also be possible to find the CO solution for which $n_A \neq n_B$. One finds that the condition for the onset of charge ordering is equivalent to $n_A = n_B = n$ being a double solution of (12). This condition is expressed as

$$n = -\frac{2}{\pi} \int_{-\infty}^{+\infty} d\omega f(\omega) \Im G(0, \omega) \quad (13)$$

$$1 = -\frac{2}{\pi} \int_{-\infty}^{+\infty} d\omega f(\omega) \Im G'(0, \omega) \quad (14)$$

where $G'(0, \omega) = \frac{\partial G(x, \omega)}{\partial x} \big|_{x=0}$ and $G(0, \omega)$ is a solution of (11) when $x = 0$. The latter is a cubic equation for $G(0, \omega)$ and the correct root must be identified from the physical condition to yield a non-negative density of states. It is also easy to obtain $G'(0, \omega)$ from eq. (11). So, for fixed temperature T , on-site Coulomb repulsion U and band filling n we have the closed system of equations (13)-(14) for the critical value V and the chemical potential μ within the framework of the CPA.

III. NUMERICAL RESULTS AND DISCUSSION

We have solved numerically eqs. (13)-(14), the results may be summarized as follows. In Fig. 1 phase diagram as a function of n and V for different values of U for the two-dimensional square lattice at zero temperature. The

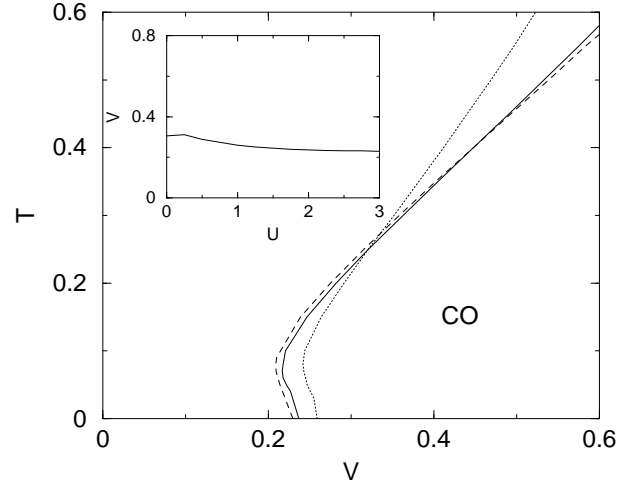


FIG. 2. $(T-V)$ -phase diagram at quarter filling for several values of U : $U = 1, 2$ and 3 corresponding the dotted, solid and dashed lines, respectively. The inset shows $(U-V)$ -phase diagram for $n = 1/2$ and $T = 0$.

half-bandwidth W was taken as unit of energy (for the square lattice $z = 4$ and $W = 4t$). Due to the electron-hole symmetry we consider only $0 \leq n \leq 1$. From Fig. 1 one can see that in the two regions ($n \ll 1$, $n \leq 1$) the influence of U on the boundary between the charge ordered and the homogenous disordered phase is different: away from half filling ($n < n^* \approx 0.67$) the on-site interaction U has little effect on the critical value V_c , while for $n^* < n \leq 1$ the critical V_c strongly depends on U . In Ref.¹⁵ Dho et al found that CO exists over a broad doping range ($0.44 \leq x \leq 0.8$) in $\text{La}_{2-2x}\text{Sr}_{1+2x}\text{Mn}_2\text{O}_7$. It is worthwhile to note that for large U in the same filling region the CPA values of V_c are close the minimum value (V_c has the minimum at $n^* \approx 0.67$). Although the mechanism of the charge ordering in the layered manganites is more complex than one induced by a nearest neighbor Coulomb repulsion, from the above result we may speculate that the CPA is able to describe the CO boundary in this compound. In addition, the advantage of the CPA is that by using this simple approach one can easily obtain phase diagrams in the $(V-n)$ -plane for arbitrary U as well as in the $(U-V)$ -plane at arbitrary n . As an illustration of our approach in the following we consider CO transition on the square lattice at quarter filling ($n = 1/2$). The inset in Fig. 2 shows the $(U-V)$ -phase diagram at zero temperature. We compare CPA result to the one obtained by other methods. At $U = \infty$ the critical value $V_c = 0.195W$ and $V_c = 0.172W$ obtained in Ref.¹⁰ by the slave boson approach with a constant and the actual DOS $\rho_0(\omega)$ respectively, is in a good agreement with our result $V_c = 0.218W$. At $U = 2W$ $V_c = 0.66W$ was obtained in Ref.⁹ for the EHM in infinite dimension by the numerical renormalization group (NRG) method, while

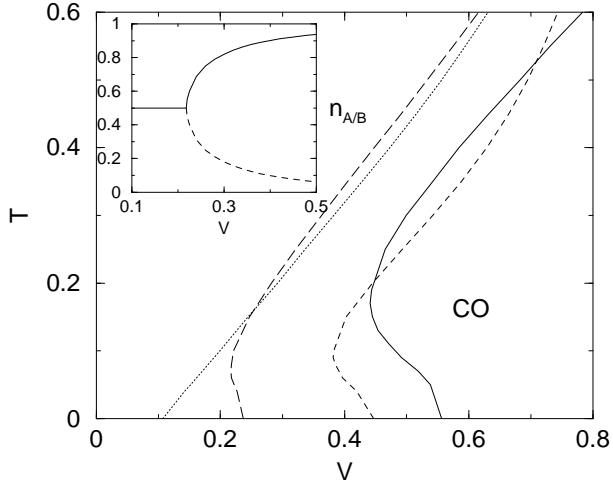


FIG. 3. $(T-V)$ -phase diagram for $U = 2$ at various values of n : $n = 0.3, 0.5, 0.65$ and 0.8 corresponding to the solid, long-dashed, dotted and dashed lines, respectively. The inset shows the lattice occupancies n_A (solid line) and n_B (dashed line) as a function of V for $U = \infty$ and $T = 0$.

the CPA result for our 2D lattice is $V_c = 0.237W$.

In Ref.¹⁰ McKenzie et al argue that in the large U limit at quarter filling the charge ordered phase is destroyed below a critical non-zero value V_c , of the order of t , while we can now show in the inset of Fig. 2 that the critical value V_c is almost independent of U , therefore V_c is of the order of t for all values of U . Fig. 2 shows the $(T-V)$ -phase diagram for different values of U . For each value of U reentrant behavior as function of temperature is seen for some region of V . For V in this range, the ground state is homogeneous but a charge ordered phase exists at intermediate temperature. Note that reentrant transition apparently is not obtained by Hartree-Fock approximation in the EHM without electron-phonon interaction. Fig. 3 shows the $(T-V)$ -phase diagram for $U = 2$ at different band fillings n . The reentrant behavior is seen clearly for the values of n where $V_c(T = 0)$ is larger (e.g. $n = 0.3, n = 0.8$), while for values of n where $V_c(T = 0)$ is small (e.g. $n = 0.65$), the reentrant behavior is not seen.

In the inset in Fig. 3 we present the CPA result for V dependence of the sublattice occupancies n_A and n_B and hence the charge order parameter $(n_A - n_B)$ in the strong correlated limit $U \rightarrow \infty$ at zero temperature. The transition is clearly continuous in contrast to the result for $U = 2, T = 0$ in Ref.⁹ where the NRG method gives a first order phase transition. Note that in the strong correlated limit $U \rightarrow \infty$ from eq. (11) one can find an analytic expression for $G(x, \omega)$. Then eqs. (12) have to be solved self-consistently to find n_A, n_B and μ . For a given set of these parameters the total energy of the system for various states can be calculated. The state with the low-

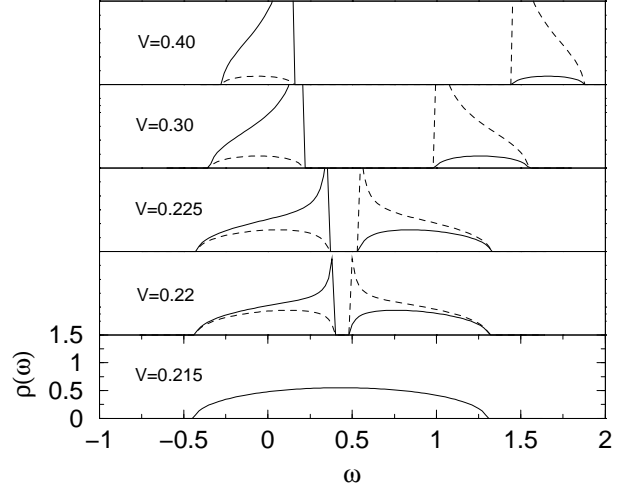


FIG. 4. CPA results at quarter filling for the A and B spectral functions $\rho(\omega)$ (solid and dashed lines, respectively) for $U = \infty, T = 0$ and several values of V . Below the critical $V_c \approx 0.218$, the spectral functions of both sublattices are equal.

est energy is the true ground state and determines the spectrum. The CPA result for A and B spectral functions for $U = \infty, T = 0$ are shown in Fig. 4. When $V < V_c \approx 0.218$ the A and B spectral functions are identical and they are independent of V by shifting all the one-electron energy levels and the chemical potential by $2V$. For $V > V_c$ the A and B spectral functions change and each spectrum splits in the upper and lower subbands. On increasing V the weight of the lower subband in the A-spectrum increases, while the one in the B-spectrum decreases; the subbands in the spectrum become narrower due to the reduced hopping of electrons in the charge ordered phase. A charge ordering gap opens and it is given by $\Delta = 2\sqrt{16V^2x^2 + \gamma}$, where $\gamma = \frac{1}{2}[(1 - \frac{n}{2}) - \sqrt{(1 - \frac{n_A}{2})(1 - \frac{n_B}{2})}]$. In the limit of large V , perfect charge order evolves: $n_A \rightarrow 1, n_B \rightarrow 0$. Therefore in this limit $x \rightarrow 1/2$ and the gap between two peaks Δ is given in CPA by $4V$, as compared to $2V$ obtained by the DMFT in Ref.⁹.

IV. CONCLUSIONS

In this paper we have applied the CPA to study charge ordering in the extended Hubbard model. Within this approximation one can obtain the critical value V_c as a function of temperature T , on-site Coulomb repulsion U and band filling n . To examine the CPA results we consider the charge ordering transition on the 2D square lattice at quarter filling using a semi-elliptical DOS. It was shown that for all values of U the charge ordered phase is

destroyed below a critical non-zero value V_c of the order of t . Like previous results in Ref.^{9,12}, we find a parameter region where the model shows reentrant behavior. The reentrant transition is also observed at other band filling, as it was experimentally found in the layered manganites in Ref.¹⁵. In the strong correlation limit $U \rightarrow \infty$ at zero temperature the CPA gives a continuous transition.

Now the CPA is known to give good results of one-particle properties in a wide range of systems. To study the CO boundary phase in the EHM the CPA has the advantage over DMFT of being analytically simple, and over Hartree-Fock approximation (small U) and slave boson approach ($U \rightarrow \infty$) of being able to describe the whole range for the on-site interaction U . Of course in common with the alloy CPA the imaginary part of the self-energy does not vanish at the Fermi level at $T = 0$, so we do not obtain a true Fermi liquid and we only expect our CPA to study CO in the EHM well at finite temperature.

The calculation presented here can also be applied to the lattice of higher dimensions, or to the EHM in the presence of a weak magnetic field. To include magnetic phases and cluster effects one has to go beyond the usual alloy CPA. This is left for our future work.

Acknowledgments

The authors would like to thank Prof. P. Fulde for useful discussions and Dr. B. Schmidt for the help in numerical calculation. This work has been done during a visit of A.T. Hoang to the MPI PKS, Dresden, whose hospitality and support are gratefully acknowledged.

-
- ¹ Wigner E 1938 *Trans. Faraday Soc.* **34** 678.
 - ² Andrei E Y *et al.* 1988 *Phys. Rev. Lett.* **60** 2765.
 - ³ Fulde P 1997 *Ann. Phys.* **6** 178.
 - ⁴ Ochiai A, Suzuki T and Kasuya T 1990 *J. Phys. Soc. Jpn.* **59** 4129.
 - ⁵ Ohama T *et al.* 1999 *Phys. Rev.* **B 59** 3299.
 - ⁶ Chen C H and Cheong S W 1996 *Phys. Rev. Lett.* **76** 4042.
 - ⁷ Seo H and Fukuyama H 1998 *J. Phys. Soc. Jpn.* **67** 2602.
 - ⁸ van Dongen P G J 1994 *Phys. Rev.* **B 50** 14016.
 - ⁹ Pietig R, Bulla R and Blawid S 1999 *Phys. Rev. Lett.* **82** 4046.
 - ¹⁰ McKenzie R H *et al.* 2001 *Phys. Rev.* **B 64** 085109.
 - ¹¹ Hirsch J E 1984 *Phys. Rev. Lett.* **53** 2327.
 - ¹² Hellberg C S 2001 *J. Appl. Phys.* **89** 6627.
 - ¹³ Tomioka Y *et al.* 1997 *J. Phys. Soc. Jpn.* **66** 302.
 - ¹⁴ Chatterji T *et al.* 2000 *Phys. Rev.* **B 61** 570.
 - ¹⁵ Dho J *et al.* 2001 *J. Phys.: Cond. Matt.* **13** 3655.
 - ¹⁶ Yuan Q and Thalmeier P 1999 *Phys. Rev. Lett.* **83** 3502.
 - ¹⁷ Hubbard J 1964 *Pro. R. Soc. London* **A 281** 401.
 - ¹⁸ Czycholl G 1986 *Phys. Reports* **143** 277.
 - ¹⁹ Vlaming R and Vollhardt D 1992 *Phys. Rev.* **B 45** 4637.
 - ²⁰ Velicky B, Kirkpatrick S and Ehrenreich H 1968 *Phys. Rev.* **175** 747.